ResearchGate

See discussions, stats, and author profiles for this publication at: https://www.researchgate.net/publication/341150466

Study of the Residual Flow and Salinity during the Spring and Neap Tides at the Seokmo Channel, South Korea

Conference Paper *in* Journal of Coastal Research · May 2016

DOI: 10.2112/SI75-285.1

CITATIONS
0

READS
56

8 authors, including:



Byung il Yoon
Inha University
29 PUBLICATIONS **183** CITATIONS
SEE PROFILE



Bon-Ho Gu
Korea Institute of Ocean Science & Technology (KIOST)
9 PUBLICATIONS **29** CITATIONS
SEE PROFILE



J.W. Kim
Inha University
21 PUBLICATIONS **81** CITATIONS
SEE PROFILE



Myung-Seok Kim
Korea Polar Research Institute (KOPRI)
22 PUBLICATIONS **91** CITATIONS
SEE PROFILE

All content following this page was uploaded by J.W. Kim on 05 May 2020.

The user has requested enhancement of the downloaded file.

Journal of Coastal Research	SI	75	1422 - 1426	Coconut Creek, Florida	2016

Study of the Residual Flow and Salinity during the Spring and Neap Tides at the Seokmo Channel, South Korea

Byung Il Yoon[†], Nakyong Choi[‡], Bon-Ho Gu[†], Jong Wook Kim[†], Jin Il Song[†], Chaewook Lim[†], Myung-Seok Kim[†], and Seung-Buhm Woo[†*]

[†]Department of Ocean Science
College of Natural Science, Inha Univesity
Incheon, South Korea

[‡]Pangyo R&D Center, Samsung Heavy Industries
Gyeonggi-do, South Korea

www.cerf-jcr.org

www.JCRonline.org

ABSTRACT

Yoon, B.I.; Choi, N.Y.; Gu, B.H.; Kim, J.W.; Song, J.I.; Lim, C.W.; Kim, M.S., and Woo, S.B., 2016. Study of the residual flow and salinity during the spring and neap tides at the Seokmo channels, South Korea. *In:* Vila-Concejo, A.; Bruce, E.; Kennedy, D.M., and McCarroll, R.J. (eds.), *Proceedings of the 14th International Coastal Symposium* (Sydney, Australia). *Journal of Coastal Research*, Special Issue, No. 75, pp. 1422 - 1426. Coconut Creek (Florida), ISSN 0749-0208.

The Seokmo (SM) channel of Gyeonggi Bay, located in the South Korea, exhibits unique and complex estuarine circulation characteristics. This study analyzed the salinity observations, and the cross-sectional variations in the residual current and strengths of stratification by tidal current, along two cross-channels transects, during the 13-hour periods of the spring and neap tides, respectively. The cross-sectional averaged residual velocity, at the northern entrance of the SM channel, showed a seaward directional flow of 0.05 m/s during the neap tide, and 0.21 m/s during spring tide. At the southern entrance, the residual current showed two-layer circulation with a landward flow in the bottom layer, and a seaward flow in the surface layer. The spatial characteristics of the landward residual current, at the southern entrance are different for the eastern and western sides of the channel, depending on the spring and neap tidal cycles. The variation in the location of the observed landward residual current, caused by the changes in spring and neap tidal cycles, and the correlation between this variation and the stratification, were analyzed using the Richardson number. At the northern and southern end of the SM channel, a landward residual current appeared in the location that Richardson number was large. These results suggested that the cross-sectional residual current pattern, at the SM channel, changes depending on freshwater and topographical influences, and is sensitive to tidal changes, such as changes in the spring and neap tidal cycles.

ADDITIONAL INDEX WORDS: *Residual current, stratification, Richardson number, Seokmo (SM) channel.*

INTRODUCTION

Gyeonggi Bay, which is located in the west coast of South Korea, is a semi-closed coastal region (Figure 1a). This estuary has a predominantly semidiurnal tide, with spring and neap tidal ranges of approximately 8.0 and 3.5 m, respectively and, due to large tidal range, the tidal flat has developed extensively. The estuarine circulation is both unique and complex, as it is connected to intricate coastlines and a high number of waterways (*e.g.*, Park *et al.*, 2002; Yoon and Woo, 2013). The seasonal variation of the freshwater discharge from the Han River has a significant effect on the estuarine circulation. The Seokmo (SM) channel, which is the key subject area of this study, has a width of 1.4 km and a length of 15.9 km, and it is located in the west of Ganghwado (Figure 1b).

The tidal residual currents in Gyeonggi Bay have been studied by Kim *et al*. (2009), Lee *et al.* (2012), and Yoon and Woo (2013). Previous studies of the SM channel have either analyzed the entire channel using a mooring point or have used numerical models, and, for this reason, it was not possible to carry out studies successfully on the overall current and salinity distribution of the channel. Therefore, the objective of our research was to understand the cross-sectional residual current characteristics, during the spring and neap tidal cycles.

METHODS

Observations of the SM channel were conducted at an interval of a 1-hour, for duration of 13 hours, over a period of 4 days, between August 24 and August 31, 2011. Regarding the observation equipment, a 600-kHz acoustic Doppler current profiler (ADCP) was used for Line 1, situated at the northern end of the SM channel (Figure 1c), and Line 2 situated at the southern end (Figure 1d). Additionally, the salinity was observed using Conductivity-Temperature-Depth (CTD) profiles at several observation stations in the SM Channel, as well as at same locations as the observation lines where the ADCP was used (Figure 1b).

The tidal ranges during the observation period, provided by the Korea Hydrographic and Oceanographic Administration, were 2.5 and 9.3 m for the neap and spring tides, respectively. Additionally, freshwater discharge data was collected in order to compare the change in magnitude of the tidal current because freshwater discharge has a significant influence on the tidal flow of the SM channel (Kim *et al.*, 2009).

DOI: 10.2112/SI75-285.1 received 15 October, 2015; accepted in revision 15 January 2016.
*Corresponding author: sbwoo@inha.ac.kr
©Coastal Education and Research Foundation, Inc. 2016

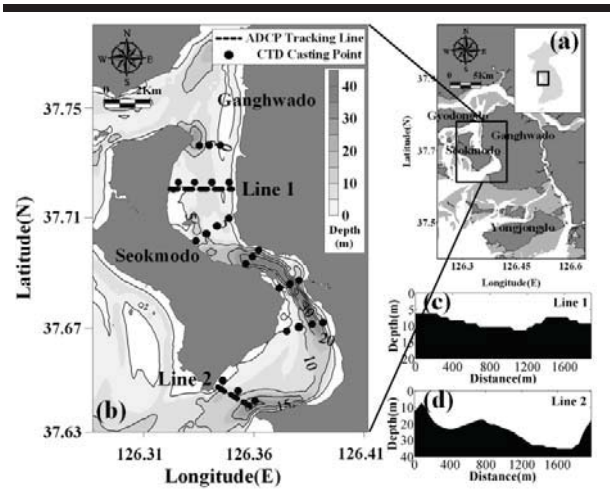


Figure 1. The study area (a) and field measurement locations of ADCP transects (b) for Lines 1 and 2. Mean depth at the north (c) and south (d) entrance of the Seokmo channel.

The ADCP raw data had a 4-stage conversion process. First, we used the method described previously by Valle-Levinson and Atkinson (1999), and obtained a single value for the averaged 10-sets of raw data. In the second stage, we removed the portion of the data which had a scale value (percent good) beam correlation of below 80% and velocity error greater than 10% of the averaged current value obtained from the averaged horizontal grid data. In the third stage, the angles were transformed. We transformed the velocities into a true north coordinate system (7-degree), and in order to correct for the vessel error, we applied the vessel speed calibration (Joyce correlation) method used by Joyce (1989). The principal component analysis is a method used to linearly transform the *u* (east-west direction) and *v* (south-north direction) components, extracted from the current data (ADCP), into a new coordinate system with longitudinal and transverse directions. This enables us to perform an analysis of the most dominant component (Preisendorfer and Mobley, 1988).

In the last stage of the data processing, we additionally transformed the data into vertical and horizontal Sigma coordinates. Due to ADCP cross-sectional observations were performed in this study area, it is difficult to construct the same grid for not only the changes in the vertical sea-level height (with respect to time, and to the spatial locations of the observations), but also for the horizontal coordinates correspond to the distance. To resolve this problem, this study included a transformation of the z-level velocities, which was verified by Lee *et al.* (2012), transforming them into a horizontal Sigma grid. Constructing a vertical and horizontal Sigma grid is useful because the entirety of the data, from all of the water layers, can be used in regions with large tides, such as the subject region of this study.

RESULTS

Figure 2 depicts the maximum flood and ebb currents during the spring and neap tides, for Lines 1 and 2. As the figure shows the cross-sections of the channel as viewed from the south, the

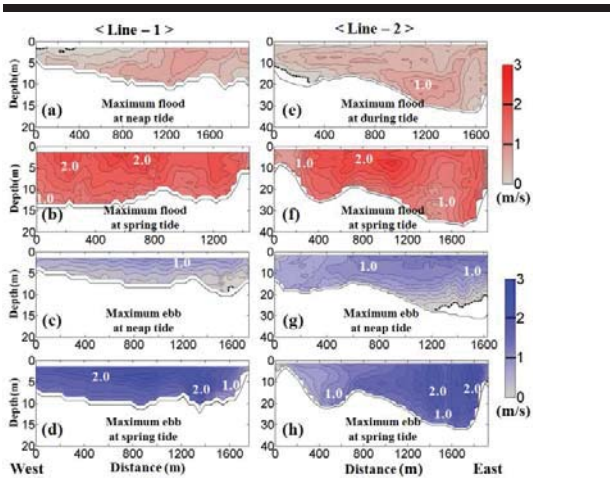


Figure 2. The along-channel current distribution at Lines 1 and 2 (towards the north). The figures on the left-hand side represent Line 1, and the figures on the right-hand side represent Line 2. The water depth (bathymetry) for (a)-(d) is difference because transects of Line 1 are difference according to spring and neap tide.

left and right sides of the figure represent the west and east directions, respectively.

For Line 1, during the neap tide, the ebb current appeared to be stronger than the flood current by more than 0.20 m/s. The maximum flood current was 0.89 m/s (Figure 2a) and maximum ebb current was 1.36 m/s (Figure 2c). Significantly higher currents were found during the spring tide, where a flood current of 1.84 m/s (Figure 2b) and an ebb current of 2.41 m/s (Figure 2d) were observed. For Line 2, a flood current of 0.98 m/s (Figure 2e) and an ebb current of 1.56 m/s (Figure 2g) were observed during neap tide, while a flood current of 2.39 m/s (Figure 2f) and an ebb current of 2.53 m/s (Figure 2h) were observed during spring tide. We found that the maximum current of Line 2 was greater than that of Line 1, but that the averaged cross-sectional current, during the spring tide, was greater for Line 1 than for Line 2.

The current at the surface layer appeared to be relatively high compared to that of the bottom layer. This was because of the bottom friction and freshwater discharge at Lines 1 and 2. In the case of Line 2, the current was relatively high on the east side compared to the west. In Line 2, the direction of the cross-section was from the south to the north, while the water flowed from the south-to-west to north-to-east directions, rather than the south-to-north direction, as was determined by the PCA analysis results (not shown).

Due to the aforementioned topographical reasons, the flow magnitude is greater than the eastern side. For the neap tide, the dotted line indicates the 0 (zero) line, classifying the region that flows in the opposite direction to the cross-sectional fluid flow. Therefore, we inferred that the flow caused by the strong

freshwater discharge is the reason why the current flows in the opposite direction, despite it being the maximum current. The SM channel is a region greatly affected by the freshwater discharge; therefore, there is a clear difference in the current distributions between the surface and bottom layers.

The M_2 and M_4 tidal components were removed from the value of each cell that was repeatedly observed, and the calculated value was defined as the residual current (Lwiza *et al*., 1991).

$$v_0 = v - \sum A_n \cos(\omega_n - \phi_n) \quad (1)$$

Here, v refers to the averaged 13-hour velocity in the axial direction (along-channel velocity), and v_0 refers to the residual velocity. A_n refers to the amplitude, ω_n refers to the angular velocity and ϕ_n refers to the phase angle. In the above equation, the v_0 value that remains after considering the phases of the M_2 and M_4 tidal components is defined as the residual current.

Figure 3 shows the cross-sectional and vertical residual current distributions at several stations located on the cross-section, during the neap and spring tides. The black dotted line in the residual current distribution plot represents the 0 m/s line, and the black dotted line in the average salinity distribution plot represents the 5 psu line. During the neap tide, at Line 1, the seaward residual current (maximum current: 0.34 m/s) was dominant through the entire surface layer due to the freshwater discharge. In the bottom layer, the landward residual current (maximum current: 0.13 m/s) was dominant.

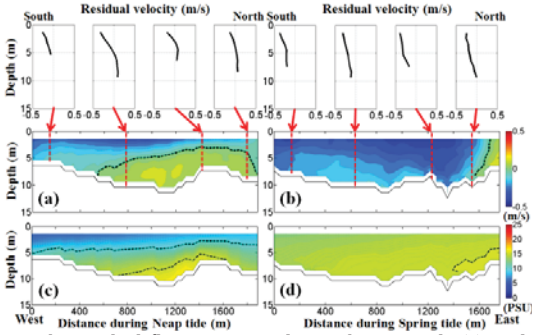


Figure 3. The residual flow at Line 1 during the neap tide (a), and the spring tide (b). The vertical profiles of the residual current at selected sites (red dotted line) in the transects are shown in the upper region of the figure. The bottom panel shows the tidally mean salinity during the observation period (c and d).

The landward residual current was found to be moving toward the east, which is on the right hand side of the channel cross-section (Figure 3a). Additionally, the averaged salinity was observed to be high in the east, which is the region where the landward residual current is illustrated (Figure 3c). The vertical structure of the residual current is different for the spring and neap tides. In the case of Line 1, during the neap tide, the ebb-directional residual current appeared in the surface layer, whereas the flood-directional residual current was strongest at the center of the cross-section.

During spring tide, the maximum landward residual current was 0.13 m/s in the bottom layer, where the averaged salinity was higher than that of the neap tide. The seaward residual current component, with a maximum velocity of 0.40 m/s, was found (Figure 3b). At this point, the landward directional residual current in the bottom layer was observed in a region further to the east, during the spring tide, than was observed during the neap tide. In contrast to the neap tide, the flood current during spring tide showed a similar distribution to that of the cross-section, whereas the ebb current was lower to the east of the channel. Therefore, the landward residual current for the spring tide was found to move more eastward than the neap tide. We hypothesized that this finding was due to the friction that resulted when the observation line at the east of the channel was not observed completely because of the tidal flat.

Similar to Line 1, the cross-sectional residual current and the averaged salinity distribution during the neap and spring tides, for Line 2, are illustrated in Figure 4. During the neap tide for Line 2, the seaward residual current of 0.54 m/s, and the landward residual current, with a maximum current of 0.43 m/s at the right hand side of the channel cross-section, are shown (Figure 4a). As in Line 1, the surface layer contained a dominantly seaward residual current, whereas a landward current, with a high salinity, was found throughout the eastern side of the channel. The residual current appeared in the eastern side of the channel, had a similar pattern of maximum current. During the spring tide, the ebb-directional residual current was observed at the eastern side of the channel, whereas a two-layer circulation pattern appeared at the western side.

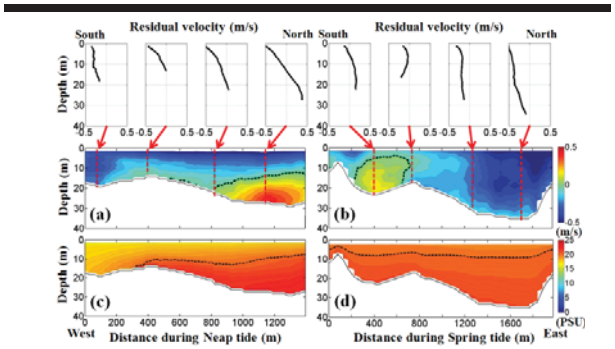


Figure 4. Same as Figure 3 but for Line 2.

During the spring tide, the landward residual current, with a maximum current of 0.22 m/s, and a seaward residual current component, with a value of 0.68 m/s, were observed (Figure 4b), and, due to mixing the salinity was evenly distributed (Figure 4d). The seaward residual current component was strongly apparent, and, unlike during the neap tide, the landward residual current component was found to be moving to the west, which is to the left hand side of the channel cross-section.

DISCUSSION

As shown from the observation results, the SM channel showed a significant difference in salinity between the northern and southern ends throughout the entire channel. In regions

similar to the SM channel, the difference in the density, due to the salinity variation, had a significant effect on the residual flow (*e.g.*, Geyer, 1987). Additionally, because the SM channel region is largely affected by freshwater discharge, when we examined the distribution of the average salinity, the two layer salinity structure was clearly apparent, as a result of the vertical salinity difference. Moreover, when we examined the distribution of the residual current, the distribution pattern of the cross-sectional residual current varied between the spring and neap tide, for Lines 1 and 2. In the case of Line 1, the landward residual current in the bottom layer, during the spring tide, appeared to occur closer to the eastern side, compared to during the neap tide, whereas, for Line 2, it appeared to occur closer to the western side during the spring tide, compared to during the neap tide. These variations suggest that the relationship between the spring and neap tides, during which the landward residual current appears, is different for Line 1 than for Line 2. In order to establish the relationship between the spring and neap tides, we analyzed the relationship between the degree of stability and the residual current during the observation period.

The stability within the cross-section of the channel can be expressed using the Richardson number (*Ri*), which is an index that represents the ratio of the buoyancy frequency (N^2) and to the stress of the vertical velocity (S^2)

$$Ri = -\frac{g}{\rho}\frac{\partial\rho/\partial z}{[(\partial U/\partial z)^2+(\partial V/\partial z)^2]} = \frac{N^2}{S^2} \quad (2)$$

Here, g refers to the gravity, ρ refers to the density, U refers to the across-channel velocity, V refers to the along-channel velocity and z refers to depth. Through experimentation and observation, a range of 0.25-0.33 was proposed as the limit of the shear instability of the *Ri* (Simpson and Briiter, 1979). If the *Ri* is less than this threshold, the shape of the stratification section appears linear, depending on the depth (Geyer, 1987). However, if the *Ri* is greater than this threshold, the direction of the velocity may appear to be different, or the difference in the velocity may be significant.

In order to compare the characteristics of the variation of the residual current in the SM Channel, the *Ri* was determined based on the observation results. Here, we applied the density value that was calculated using the salinity value that was observed from the CTD profiles. In addition, both the current and density are required to find the *Ri*, and the current value used here to find the *Ri* is the current that corresponds to the location of the CTD observation.

Figure 5 illustrates the *Ri*, in addition to the distribution of the residual current. When the *Ri* value is significantly changed, the direction of the current changes (Framinan *et al*., 2008). It was suggests that the change in the residual current has a significant influence on the change in stratification (Prandle, 1981). In regions where the flood-directional residual current appears in the bottom layer, we can see that the *Ri* becomes abnormally large. Similar results were found for both Line 1 and Line 2 during the neap tide as well as during the spring tide. Because this comparison is between the *Ri* for 1 hour and the residual current, we cannot use the threshold used in previous studies. However, this result still shows that the region in the bottom layer, where the landward residual current occurs is very unstable.

The *Ri* becomes larger when the landward residual current in the bottom layer is observed for all flood tides. However, low *Ri* values were observed at a point 1400 m from the western side of the channel during the ebb tide of the neap period and a point 1600 m from the western side of the channel during the ebb tide of the spring period even though a landward residual current occurred in the bottom layer. This phenomenon occurred because there was no stratification during the ebb tide; however, stratification did occur during the flood tide, causing the formation of a landward residual current in the bottom layer. Additionally, during the neap period, when we found that the *Ri* became significantly large at the center of channel during the flood tide, and that the *Ri* became significantly large in the eastern side of the channel during ebb tide, the unstable velocity pattern, during the flood and ebb tides, was found to have moved from the center to the eastern side of the channel. This result indicates that the levels of instability in the stratification and velocity were different for the flood and the ebb tides.

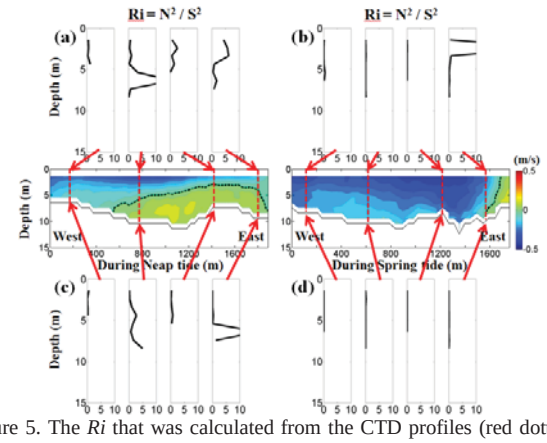


Figure 5. The *Ri* that was calculated from the CTD profiles (red dotted line) for Line 1. The results during neap and spring tides are shown in the left and right panel, respectively, during the flood tide: (a) and (b), and ebb tide: (c) and (d). For comparison, the residual velocity is shown in the center of the figure (flowing towards the north).

Figure 6 shows the *Ri* and residual currents for Line 2, in the same way as it was shown for Line 1. In the region where the landward residual current occurs in the bottom layer, with respect to the channel cross-section, the *Ri* is large and unstable. A large *Ri* was found in the region with a landward residual current in the bottom layer during the spring tide; however, during the neap tide, the *Ri* value was large in the western side, despite the fact that the landward residual current was not observed. The reason for this is that, for Line 2, the current appeared to be greater in the western side of the cross-section than in the eastern side; therefore, the *Ri* value was greater. This finding also demonstrated that the change in the vertical stability, in the transverse direction within the cross-section, was much greater during the neap tide than during the spring tide.

As shown in previous studies comparing the stability and the residual current, the comparison between the *Ri* and the residual current, in this study, demonstrated that in a region with a large *Ri*, the residual current for the channel cross-section presents different patterns in the surface layer than in the bottom layer.

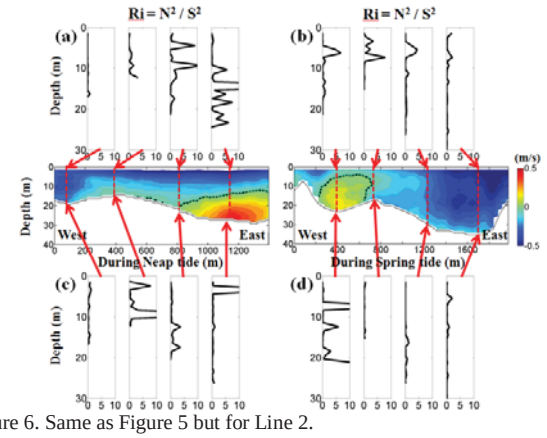


Figure 6. Same as Figure 5 but for Line 2.

Although the stability was not likely to be the reason for the occurrence of a landward residual current into the bottom layer as observed via a cross-sectional observation, one of the characteristics of the residual current that changes in the SM channel is exhibited through the stability.

CONCLUSIONS

In this study, the cross-sectional current and salinity distributions were observed during a continuous 13-hour period, at 2 different cross-sections which located at the northern and southern ends of the SM channel, South Korea. The residual current component, in the cross-section at the northern end of the SM channel, showed a seaward flow, whereas landward flows were found at the southern end. However, a landward residual current was observed in the bottom layer in every channel cross-section, thus clearly indicating a two-layer circulation structure.

As a result of analyzing the *Ri*, which is an index that represents the stability of the channel cross-section, we found that it increased in regions where the landward residual current appeared in the bottom layer during both the flood and ebb tides. These results indicated that in some regions of the cross-section, the stratification is stronger where vertical mixing does not actively occur. Thus, we cannot state that the stratification is the reason for the varying distribution patterns of the landward residual current in the bottom layer at the northern and southern ends of SM channel. However, using this analysis, we found that the landward residual current in the bottom layer occurred at a value which represents the stratification.

ACKNOWLEDGMENTS

This research was a part of the project titled ‘Development of integrated estuarine management system’, funded by the Ministry of Oceans and Fisheries, Korea. Additionally, this work was supported by INHA UNIVERSITY Research Grant.

LITERATURE CITED

Framinan, M.; Valle-Levinson, A., and Sepulveda, H. 2008. Tidal variations of flow convergence, shear, and stratification at the Rio de la Plata estuary turbidity front. *Journal of Geophysical Research*, 113(C8), 1-17.

Geyer, W.R. and Smith, J.D., 1987. Shear instability in a highly stratified estuary. *Journal of Physical Oceanography*, 17(10), 1668-1679.

Joyce, T.M., 1989. On in situ “calibration” of shipboard ADCPs. *Journal of Atmospheric and Oceanic Technology*, 6(1), 169-172.

Kim, C.S.; Lim, H.S.; Kim, J.A., and Kim, S.J., 2009. Residual flow and its implication to macro-tidal flats in Kyunggi Bay estuary of Korea. *Journal of Coastal Research*, Special Issue No. 56, 976-980.

Lee, D.H.; Yoon, B.I.; Kim, J.W.; Gu, B.H., and Woo, S.B., 2012. The cross-sectional mass flux observation at Yeomha channel, Gyeonggi Bay at spring tide during dry and flood season. *Jouranl of Korean Society of Coastal and Ocean Engineers*, 25(1), 16-25.

Lwiza, K.M.M.; Bowers, D.G., and Simpson, J.H., 1991. Residual and tidal flow at a tidal mixing front in the North Sea. *Continental Shelf Research*, 11(11), 1379-1395.

Park, K.; Oh, J.-H.; Kim, H.-S., and Im, H.-H., 2002. Case study: mass transport mechanism in Kyunggi Bay around Han River mouth, Korea. *Journal of Hydraulic Engineering*, 128(3), 257-267.

Prandle, D., 1981. Salinity intrusion in estuaries. *Journal of Physical Oceanography*, 11(10), 1311-1324.

Preisendorfer, R.W. and Mobley, C.D., 1988. Principal component analysis in meteorology and oceanography. *Developments in Atmospheric Science*. Amsterdam, 425p.

Simpson, J.H. and Britter, R., 1979. The dynamics of the head of a gravity current advancing over a horizontal surface. *Journal of Fluid Mechanics*. 94(3), 477-495.

Valle-Levinson, A. and Atkinson, L.P., 1999. Spatial gradients in the flow over an estuarine channel. *Estuaries*, 22(2), 179-193

Yoon, B.I. and Woo, S.B., 2013. Tidal asymmetry and flood/ebb dominance around the Yeomha channel in the Han River Estuary, South Korea. *Journal of Coastal Research*, Special Issue No. 65, 1242-1246.

View publication stats